

Article

Photovoltaic Inverter Profiles in Relation to the European Network Code NC RfG and the Requirements of Polish Distribution System Operators

Krzysztof Chmielowiec *, Łukasz Topolski *, Aleks Piszczek and Zbigniew Hanzelka

Department of Power Electronics and Energy Control Systems, Faculty of Electrical Engineering, Automatics, Computer Science and Biomedical Engineering, AGH University of Science and Technology, 30-059 Kraków, Poland; apiszczek@student.agh.edu.pl (A.P.); hanzel@agh.edu.pl (Z.H.)

* Correspondence: kchmielo@agh.edu.pl (K.C.); topolski@agh.edu.pl (Ł.T.)

Abstract: The presently observed rapid increase in photovoltaic (PV) micro-installation connections to low-voltage networks, resulting from numerous financial support programmes, European Union (EU) energy policy and growing social awareness of environmental and economic issues, raise the question if PV inverters widely available in EU market fulfil the numerous technical requirements specified in European and Polish regulations. The paper presents the results of an experimental study carried out on three PV Inverters widely available in the EU in accordance with the EU network code NC RfG, standard EN 50549-1:2019 and internal Polish distribution system operators' (DSOs') regulations, governing PV inverter cooperation with the low-voltage distribution network. The laboratory test stand scheme and its description are presented. In each test, at least one of the inverters encountered issues, either with the operation in required frequency ranges (one PV inverter), activating reactive power control modes (all three PV inverters), maintaining required power generation gradient after tripping (one PV inverter) or under-voltage ride through immunity (one PV inverter). The obtained results have shown that all tested PV inverters did not meet requirements that are the key to maintaining reliable and safe operation of transmission and distribution electrical networks.

Keywords: photovoltaic (PV) micro-installations; PV inverter; EU network code NC RfG; standard EN 50549-1:2019



Citation: Chmielowiec, K.; Topolski, Ł.; Piszczek, A.; Hanzelka, Z. Photovoltaic Inverter Profiles in Relation to the European Network Code NC RfG and the Requirements of Polish Distribution System Operators. *Energies* **2021**, *14*, 1486. <https://doi.org/10.3390/en14051486>

Academic Editor: Alessandro Massi Pavan

Received: 30 December 2020
Accepted: 26 February 2021
Published: 9 March 2021

Publisher's Note: MDPI stays neutral with regard to jurisdictional claims in published maps and institutional affiliations.



Copyright: © 2021 by the authors. Licensee MDPI, Basel, Switzerland. This article is an open access article distributed under the terms and conditions of the Creative Commons Attribution (CC BY) license (<https://creativecommons.org/licenses/by/4.0/>).

1. Introduction

Steadily increasing electricity prices [1] associated with increasing electrical energy consumption [2–4], the necessity for the reduction of greenhouse gas emissions included in EU policies regarding climate protection [5,6] and rapid technological development in power electronics and numerous programmes in EU member states, supporting the development of renewable energy sources (RESs) and low-carbon technologies, mean that in recent years the exponential trend of installed photovoltaic (PV) micro-installation capacity has been observed.

For Poland, regarding the Renewable Energy Directive 2009/28/EC [7], a national overall target for the share of RESs in gross final energy consumption in 2020 amounting to 15% was specified. In November 2016, the European Commission published its “Clean Energy for all Europeans” package [8]. As a part of this package, the Commission adopted a legislative proposal for a recast of the Renewable Energy Directive. In December 2018, after a final compromise among the EU institutions, the revised Renewable Energy Directive 2018/2001/EU (RED II) [9] entered into force. In the RED II document [9], the overall EU target for RES consumption by 2030 was raised to 32%. In order to meet EU obligations, the expansion of RESs in Poland was placed high on the public agenda.

Therefore, in years 2014–2020, the Polish National Fund for Environmental Protection and Water Management developed several priority programmes [10–15] addressed to

Polish families, which provide financial support for construction of photovoltaic micro-installations on the rooftops of their houses. One of those priority programmes, “My Electricity” [11–15], which is one of the biggest financial support programmes in Europe, with a budget over EUR 240 million, has contributed to the connection of over 1.2 GWp in photovoltaic micro-installations to low-voltage networks since its beginning in September 2019 [14]. Total registered applications by the Polish National Fund for Environmental Protection and Water Management for co-financing of PV micro-installations in two editions of the programme exceeded 260,000. Over 650 MWp of PV micro-installations were connected to the network, with an average power of 5.7 kWp [15]. Despite the closure or restriction of activities in some sectors of the economy due to the COVID-19 pandemic, the PV industry has not slowed down, quite the contrary. Installed capacity in Poland at the end of 2020 exceeded 3.5 GW, whereas at the end of 2019 it was almost 1.5 GW. This means an annual increase of over 150%. Poland has become the 4th market in the EU and aspires to be in the top 10 of global markets. In Figure 1 is shown the cumulative diagram of total installed capacity and the number of photovoltaic micro-installations in Poland in years 2013–2020 (till 30 September 2020).

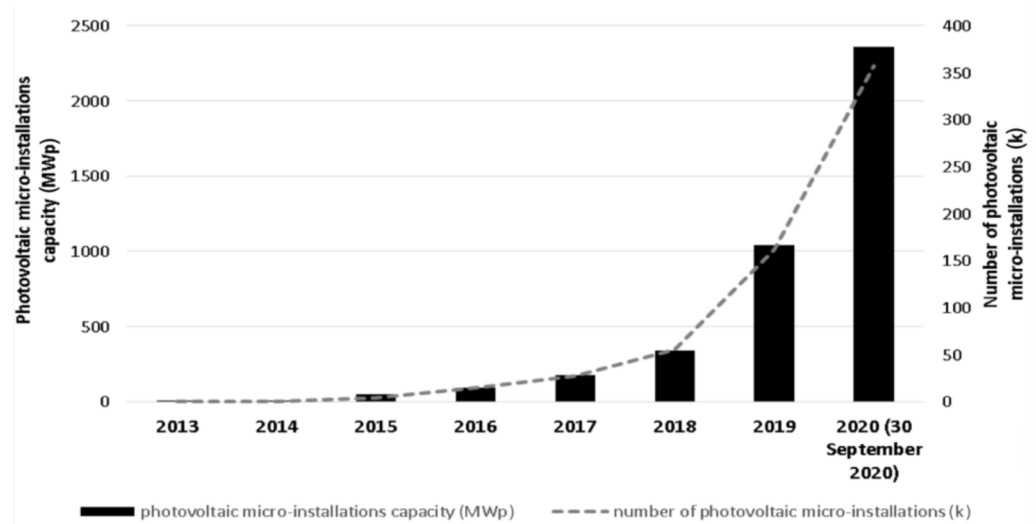


Figure 1. Cumulative diagram of total installed capacity and the number of photovoltaic micro-installations in Poland (years 2013–2020) [16].

Due to the observed huge growth of installed photovoltaic micro-installations in Poland, in some low-voltage networks, energy from PVs became the main factor determining the energy flow direction, voltage levels and their imbalance. This mainly concerns rural low-voltage networks, which are characterised by low-load profile in noon hours (high generation hours), long low-voltage feeders (up to 1 km) and small cross-sections of conductors (predominantly these are bare aluminum conductors of 50 mm²). As a result, in combination with a high simultaneous energy generation coefficient (often close to 1), photovoltaic micro-installations significantly increase the RMS (root-mean-square) voltage at the point of common coupling above 253 V, a permissible limit for the low-voltage networks specified in [17], which trips the micro-installations’ overvoltage protection system. This is often the main reason for complaints to distribution system operators (DSOs) from surprised prosumers who expect full production of electricity from photovoltaic micro-installations on a sunny summer day.

Besides voltage rise, photovoltaic micro-installations can also cause other negative impacts on distribution networks. In references [18–20], there are listed the most common issues of PV distributed generation, which include:

- Phase voltage and current imbalance (mainly regarding single-phase PV micro-installations);

- Reverse power flow (radial electrical networks have been designed to withstand unidirectional power flow, so reverse power flow can lead to distribution line overload and can also be problematic for protection devices);
- Increased power losses (which applies to a situation where reverse power flow occurs in radial low-voltage networks for which downgrading of the cross-section of conductors along feeders was applied);
- Current distortion (current harmonics distort the waveform of supply voltage, which can lead to malfunction of protection devices and also cause increased power losses in power lines and transformers).

The photovoltaic inverter is the heart of any photovoltaic micro-installation responsible for the DC-AC conversion of current and voltage, therefore, many concerns are focused on its operation, because its design quality may have significant influence on the safety, performance and reliable operation of the power system and power quality at the point of common coupling in low-voltage networks. In order to ensure appropriate operation of photovoltaic inverters, in the point of view of transmission system operators (TSOs) and DSOs, including limiting the phenomenon of increasing the RMS voltage caused by the generation of electrical energy, a number of requirements have been formulated for micro-installations, which are specified in the EU network code NC RfG [21], the standard EN 50549-1:2019 [22] and the internal document of Polish DSOs [23], which are presented and described in Section 2.

An important provision of the EU network code NC RfG [21], regarding the process of connecting type A power-generating modules (in Poland, these are modules with a capacity up to 200 kW, including micro-installations), is the requirement put on prosumers of submitting to DSOs the so-called “equipment certificate”. This is a document issued by an entity with accreditation given by the national affiliate of the European co-operation for Accreditation (EA), confirming that a given power-generating module meets the requirements of the EU network code NC RfG [21]. However, this provision will apply in Poland after 27 April 2021, due to the present lack of developed rules and procedures for such certification. Up to this date, declarations of conformity issued by the equipment manufacturer are valid. This situation, during the transitional period, can mean that manufacturers, driven by the desire for a quick profit, can issue “empty” declarations of conformity to get access and sell their products in EU member states.

Furthermore, in references [24–29], different desired requirements of PV inverters are discussed. Reference [24] reviews and analyses existing voltage control methods to improve voltage regulation and to increase hosting capacity in low-voltage networks. The authors of the paper propose a coordinated voltage control method, where the local controllers of each PV inverter use reactive power control mode $Q = f(U)$ and, if necessary, the active power curtailment $P = f(U)$ based on the local voltage measurement and the predetermined settings calculated by the supervision control unit. Performed simulations showed that the advantage of this method is that the calculated reactive power and the active power droop settings allow a fair contribution of each PV inverter to the voltage regulation. In reference [25], the authors review various reactive power control methods and propose a centralised reactive power management and coordination of modified reactive power control mode $Q = f(U)$ for allocating the reactive power to PV systems. Performed simulations showed that the proposed method can regulate voltages better than the regulation based on non-centralised reactive power control using standard $Q = f(U)$ characteristics. In reference [26], the authors give an overview on the necessary features of grid-connected inverters, which according to the German grid codes, should contribute to:

- Reactive power exchange and voltage control;
- Under-voltage ride through (UVRT) support in case of balanced faults;
- Defined behavior in case of unbalanced faults;
- Post-fault active power recovery.

Performed simulations showed that the implemented abovementioned additional abilities of the grid-connected inverters improved power quality at the point of connection

and contributed to their safety and smooth operation. In reference [27], the authors, in terms of the Horizon 2020 InterFlex project, conducted research on increasing micro-installation hosting capacity in low-voltage networks by activating reactive and active power control characteristics in PV inverters. The authors conducted theoretical and practical analysis in three selected low-voltage networks located in the Czech Republic. The obtained results showed that activating the abovementioned characteristics can increase hosting capacity from 20% to 60% depending on feeder electrical parameters and micro-installation placement along the feeder. The Czech Republic DSO plans to take action to implement control functions in its network code. In reference [28], the authors propose a control system for PV inverters to increase the UVRT immunity in a high X/R network ratio. Performed simulations showed that the injection of active power into the network during voltage sag operation improves the voltage profile at the point of PV inverter connection. In reference [29], the authors review various national grid code requirements for UVRT immunity (e.g., Poland, Spain, Germany, Italy and the United Kingdom). The authors noticed that requirements for UVRT immunity vary from country to country. A common feature is that almost all of the selected countries have defined the minimum recovery time and duration of PV inverters staying connected to the network during fault occurrence. The authors also concluded that inverter manufacturers are facing numerous challenges in the design and implementation of active and reactive power control methods to fulfil different (for each country) UVRT requirements. In reference [30], the authors propose a new passive islanding detection technique based on the rate of change of voltage (ROCOV) and the ratio of voltage and current magnitudes (VOI) in order to detect all kind of events and distinguish them from islanding conditions. The authors performed simulations of islanding events and non-islanding events, such as a single-phase or three-phase to ground fault, a sudden connection of loads and capacitor bank switching on. The obtained results showed that the proposed method can correctly distinguish islanding conditions from other events that can occur in the network. The authors also highlight that the proposed method can be easily implemented in PV inverters or in protection systems of distribution networks.

The authors of this paper would like to highlight that there is a small and insufficient number of publications that describe and analyse practical research on requirements of PV inverters with accordance to the EU network code NC RfG [21] and the standard EN 50549-1:2019 [22]. Only in reference [31] have the authors carried out similar research, but limited only to the active power response to overfrequency in a power system (which is briefly described in Section 3.1). This is only one of many other requirements that are specified in documents [21,22]. Due to this fact, the authors have decided to fill this gap and conduct practical experiments on selected PV inverters according to the most important requirements presented in documents [21,22], the fulfilment of which should contribute to the reliable and safe operation of transmission and distribution electrical networks.

2. Selected Requirements for Photovoltaic Inverters

2.1. Operating Frequency Requirements

According to the provisions of the EU network code NC RfG [21], the standard EN 50549-1:2019 [22] and the Polish DSOs' document [23], Table 1 presents the requirements for the operation of photovoltaic inverters in different frequencies, deviating from a nominal value, without disconnecting from the network.

According to Table 1, only for the frequencies in the range of 49.0–51.0 Hz is continuous operation of the photovoltaic inverter required. The standard [22], in addition to the minimum requirements, also specifies stringent requirements, the fulfilment of which may be required by some TSOs or DSOs under operation of photovoltaic inverters in certain synchronous areas or connected to small isolated distribution networks (typically on islands). Nevertheless, they are expected to be within the boundaries of the stringent requirements, as indicated in Table 1, unless the manufacturer, TSO, DSO or responsible party agrees on wider frequency ranges and longer durations.

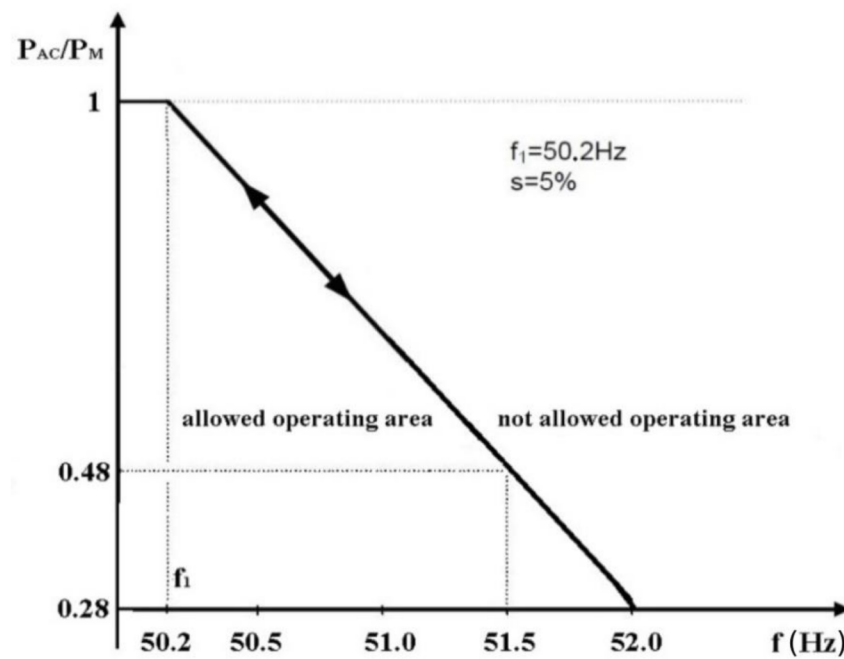
Table 1. Minimum time periods for operation in underfrequency and overfrequency for photovoltaic inverters [21–23].

Frequency Range	Time Period for Operation	
	Minimum Requirements [21–23]	Stringent Requirements [22]
47.0–47.5 Hz	not required	20 s
47.5–48.5 Hz	30 min	90 min
48.5–49.0 Hz	30 min	90 min
49.0–51.0 Hz	unlimited	unlimited
51.0–51.5 Hz	30 min	90 min
51.5–52.0 Hz	not required	15 min

Besides the requirements for operation in a wide range of frequencies, photovoltaic inverters shall also be capable of operating in so-called “limited frequency sensitive mode—overfrequency” (LFSM-O) mode, which will result in an active power output reduction in response to a change in the system frequency above a certain value. Photovoltaic inverters shall be capable of activating [21–23]:

- active power response to overfrequency at a programmable frequency threshold f_1 at least between and including 50.2 Hz and 52 Hz (default value $f_1 = 50.2$ Hz);
- a programmable droop s in a range of at least 2–12% (default value $s = 2\%$).

In Figure 2 is shown an example of the required characteristic of active power frequency response to overfrequency.

**Figure 2.** Required active power frequency response to overfrequency for photovoltaic inverters [22].

As shown in Figure 2, it is required to reduce the P_{AC}/P_M active power generation in response to the increase in the network frequency f . The reduction of the active power generation shall not exceed the allowed operating area.

The required value of the generated active power P_{AC} at the output of the photovoltaic inverter at the actual network frequency f can be determined based on the equation [22]:

$$P_{AC} = P_M + \Delta P = P_M + \frac{1}{s} \frac{(f_1 - f)}{f_n} P_M = P_M \left(1 + \frac{1}{s} \frac{(f_1 - f)}{f_n} \right) \quad (1)$$

The symbols used in Figure 2 and Equation (1) correspond to: P_{AC} —required active power at the output of the photovoltaic inverter (W); P_M —active power generated at the output of the photovoltaic inverter at the network frequency f_1 (W); f_1 —LFSM-O mode threshold activation (Hz); f —actual network frequency (Hz); f_n —nominal network frequency (Hz); s —programmable droop (%).

2.2. Reactive Power Control Mode Requirements

According to the standard [22] and the internal Polish DSOs' document [23], photovoltaic inverters shall have the capability of managing reactive power in a wide range of normal operation. Photovoltaic inverters shall respond to the RMS voltage changes and avoid exceeding RMS voltage limits permissible for low-voltage networks. In Figure 3 is shown the permissible range of reactive power control during the generation of active power by a photovoltaic inverter in a four-quadrant coordinate system.

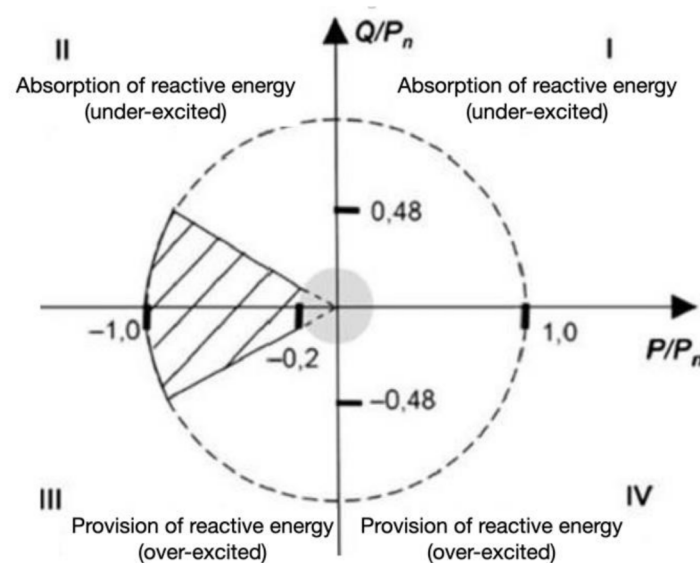


Figure 3. Permissible range of reactive power control for photovoltaic inverters in Poland [23].

The general requirement resulting from documents [22,23] states that the reactive power control shall be within the displacement power factor $\cos\varphi$ ranging from 0.9_{ue} (under-excited) to 0.9_{oe} (over-excited), while actual generating active power P is greater or equal to 20% of the nominal photovoltaic inverter active power P_n , as is shown in Figure 3.

The documents [22,23] also state that photovoltaic inverters shall be capable of operating in the following reactive power control modes:

- $Q = f(U)$ —this is the voltage-related control mode, which controls the reactive power output Q as a function of the RMS voltage U . According to the internal Polish DSOs' document [23], operation in $Q = f(U)$ control mode shall be performed in accordance with the characteristics shown in Figure 4.

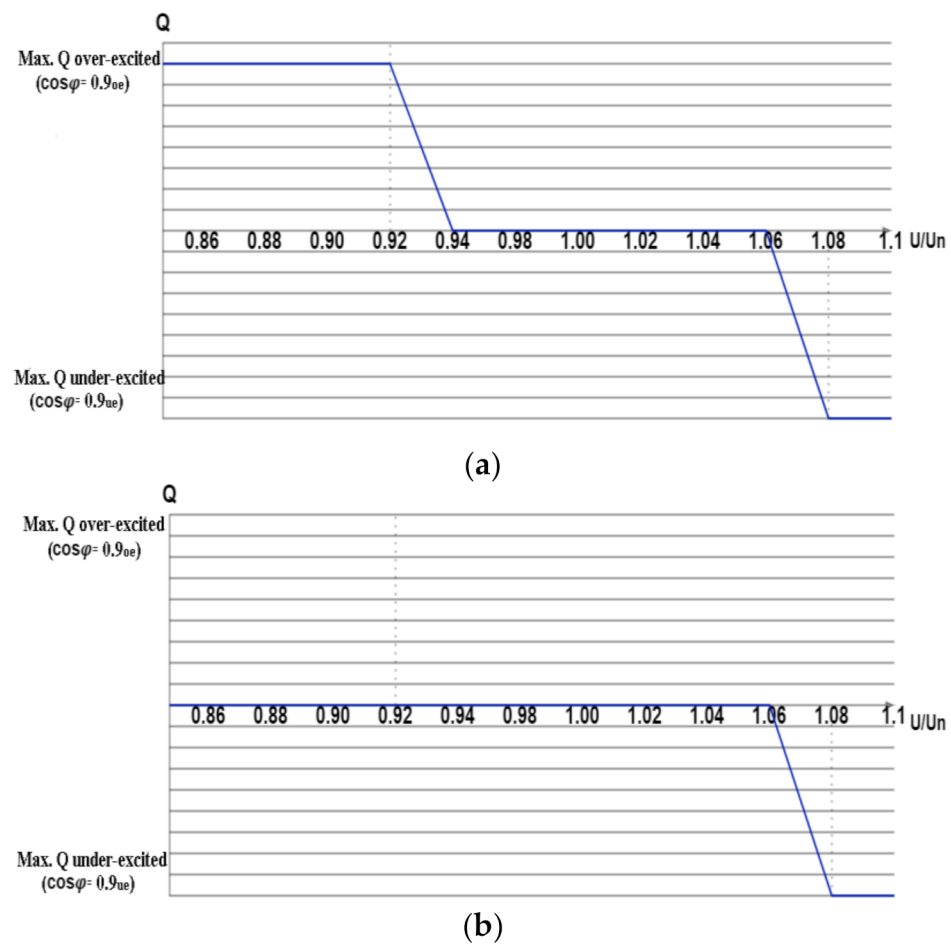


Figure 4. Required reactive power control characteristics as a function of the root mean square (RMS) voltage for three-phase (a) and single-phase (b) inverters in Poland [23].

Operating in $Q = f(U)$ control mode, in the case of an increase in the RMS voltage at the photovoltaic inverter's terminals in the range of 6–8% of the nominal RMS voltage, the inverter shall linearly increase the reactive power absorption (under-excited) in order to reduce the RMS voltage at its terminals. For three-phase inverters, it is also required that in the case of a decrease in the RMS voltage at the inverter's terminals, in the same range as for the RMS voltage increase, the inverter shall linearly increase the reactive power provision (over-excited) in order to raise the RMS voltage at the point of the inverter connection.

- $\cos\phi = f(P)$ —this is the generated active power related mode, which controls the output displacement power factor $\cos\phi$ as a function of the generated active power output P . According to the internal Polish DSOs' document [23], operating in $\cos\phi = f(P)$ control mode shall be performed in accordance with the characteristic shown in Figure 5.

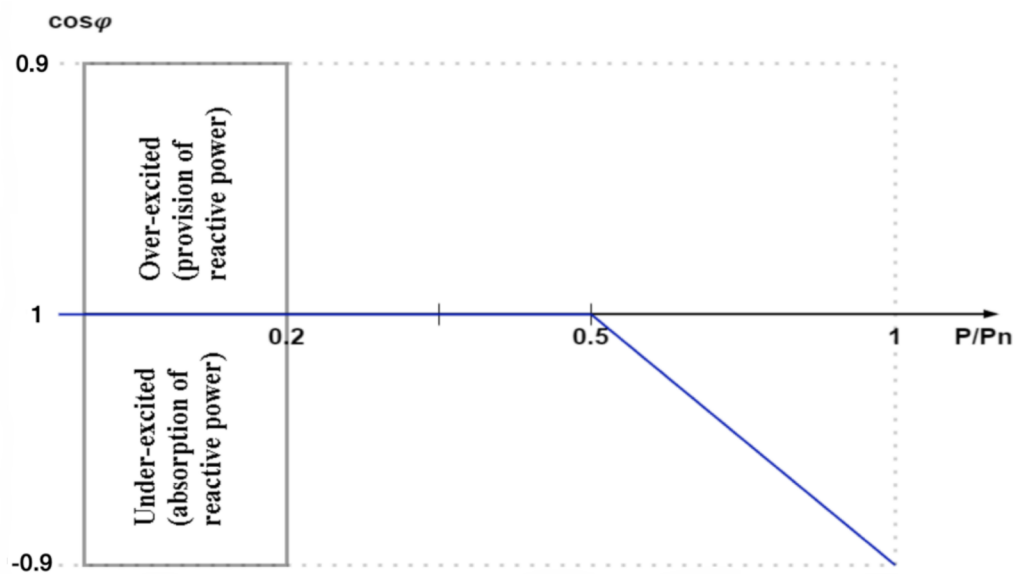


Figure 5. Required displacement power factor $\cos \varphi$ control characteristic as a function of the active power generation for inverters in Poland [23].

As is shown in Figure 5, after the photovoltaic inverter exceeds half of its nominal active power, the inverter shall linearly increase the reactive power absorption (under-excited), reducing displacement power factor $\cos \varphi$ from 1 to 0.9, regardless of the RMS voltage at the inverter terminals.

- $\cos \varphi$ setpoint mode—this is the control mode that controls the output displacement power factor $\cos \varphi$ according to a setpoint set in the control of the photovoltaic inverter;
- Q setpoint mode—this is the control mode, similar to the $\cos \varphi$ setpoint mode, that controls the output reactive power according to a setpoint set in the control of the photovoltaic inverter.

The configuration, activation and deactivation of the abovementioned control modes shall be field adjustable. It is also required that manufacturers of the photovoltaic inverters protect the settings from unpermitted interference by, e.g., a password or seal. A list of the control modes which are available in a product and how they are configured shall be stated in product documentation [22,23].

If operation of the photovoltaic inverter in one of the reactive power control modes does not contribute to the voltage reduction, documents [22,23] allow reducing active power output as a function of the voltage rise, i.e., activating $P = f(U)$ control mode. The final implemented logic can be chosen by the manufacturer. Nevertheless, this logic shall not cause steps or oscillations in the active power output [22,23].

2.3. Requirements on Under-Voltage Ride Through Immunity

Under-voltage ride through (UVRT) requirements are defined in the EU network code NC RfG [21] for type B, type C and type D power-generating modules (in general, these are power-generating modules of capacity above 200 kW and are not in the scope of this study), but are not mentioned for type A modules. Nevertheless, UVRT is seen as an important requirement in some EU member states even for small modules, such as type A. For these reasons, in the standard [22], the UVRF functionalities for type A modules are not defined as requirements (shall) but as recommendations (should).

According to the standard [22], type A power-generating modules should be capable of remaining connected to the distribution network as long as the network voltage remains above the curve shown in Figure 6. After the voltage returns to normal conditions, 90% of pre-fault power (or available power, whichever is the smallest) should be resumed as fast

as possible, but not later than 1 s unless the DSO and responsible party requires another value.

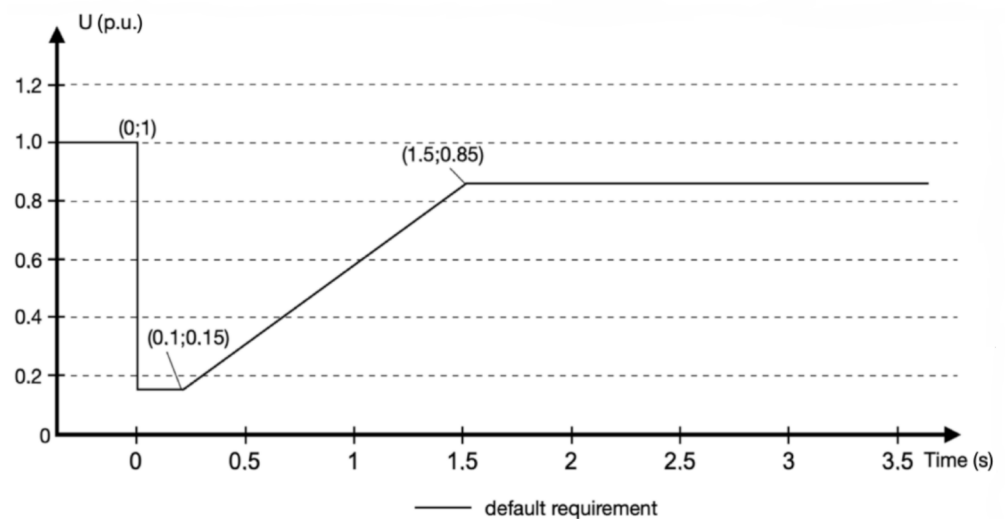


Figure 6. Under-voltage ride through capability recommendation for type A modules [22].

The UVRT capability is particularly important for TSOs, which are responsible for reliable and stable national network operation.

An example of the importance of the immunity to rapid voltage sags is the big power outage that occurred in the United Kingdom (UK) on 9 August 2019. It was the worst blackout for a decade where over 1 million people went without the power for 45 min [32,33]. The problem began when lightning struck a 400 kV overhead transmission line that caused a 737 MW large offshore wind farm disconnection after 0.3 s due to a voltage disturbance (deep voltage sag of 44% magnitude and 100 ms duration). Next, that sudden loss of power caused a steep network frequency drop which led to the disconnection of a 641 MW gas power station and 500 MW capacity of small distributed generation (due to island protection tripping). The UK National Regulatory Authority OFGEM concluded that the 737 MW offshore wind farm did not remain connected after the lightning struck, which initiated the sequence of events [34].

This recent event shows the importance of immunity to voltage sags, even if the duration of that event is short. With increasing reliance on wind and photovoltaics, new stability and reliability problems can be expected in the future because of decreasing short-circuit capacities and power system moment of inertia. This also applies to photovoltaic micro-installations (type A power-generating modules) because short-lasting deep voltage sags on high- or medium-voltage distribution lines could also lead to the disconnection of significant distributed generation capacities.

2.4. Requirements on Rate of Change of Frequency (ROCOF) Immunity

The rate of change of frequency (ROCOF) immunity of a power-generating plant means that the generating modules are able to operate properly when the frequency in the distribution network changes with a specific ROCOF value. The generating modules shall have ROCOF immunity for a ROCOF equal or exceeding the value specified by the responsible party. If no ROCOF immunity value is specified, the following ROCOF immunity shall apply [22]:

- Non-synchronous generating technology (e.g., connected to the network through power electronics): at least 2 Hz/s;
- Synchronous generating technology: at least 1 Hz/s.

The requirements resulting from the internal Polish DSOs' document [23] states that for photovoltaic inverters connected to low-voltage networks, the ROCOF immunity value shall be equal to 2.5 Hz/s.

The ROCOF protection is used as an anti-islanding protection, which is based on the local voltage measurement and estimation of the rate of change of network frequency. Then, the measured rate of change of network frequency is compared with the preset value. The ROCOF immunity is defined with a sliding measurement window of 500 ms [22].

2.5. Requirements on Protection System

According to the internal Polish DSOs' document [23], each photovoltaic shall be equipped with a protection system with parameters as shown in Table 2.

Table 2. Required photovoltaic inverter protection system, its thresholds and tripping times by Polish distribution system operators (DSOs) [23].

Protection Function	Threshold	Maximum Tripping Time
voltage drop	195.5 V	1.5 s
voltage rise—stage 1 ¹	253 V	3.0 s
voltage rise—stage 2	264.5 V	0.2 s
frequency drop	47.5 Hz	0.5 s
frequency rise	52 Hz	0.5 s
island operation detection	2.5 Hz/s	0.5 s

¹ A 10 min mean RMS value calculated as the square root of the arithmetic mean of the squared input values over 10 min. A 10 min mean RMS value is calculated in a moving window, refreshing every 3 s.

Voltage rise protection (both stages 1 and 2) is especially important for DSOs because it is the first line to protect the low-voltage network and consumers' equipment from hazardous voltage rises.

According to the documents [22,23], automatic reconnection after tripping shall be preceded by the fulfilment of the following conditions simultaneously:

- The system frequency shall be in the range of 49.5–50.2 Hz;
- The RMS voltage shall be in the range of 195.5–253 V;
- The active power generation rise shall not exceed a gradient of 10% of the inverter nominal active power per minute.

Automatic reconnection after tripping can only take place after fulfilment of the abovementioned conditions and the minimum observation time of 60 s [22,23].

3. Photovoltaic Inverters, Experimental Platform Setup and Test Results

This study is performed on three PV inverters of two manufacturers, both from outside the EU. These were low-price devices (ca. EUR 450 for the single-phase and ca. EUR 900 for the three-phase PV inverter), which are quite popular and widely available on Polish and EU markets. They were made available for the purpose of this research by a local PV installer and prosumer, and both had some doubts about their quality and performance and were unable to judge these on their own. All tested inverters were labelled with CE marking and had a declaration of conformity with the EU network code NC RfG [21] and the standard EN 50549-1:2019 [22]. Inverters X and Y were configured to operate in accordance with the Polish Grid Code (user interface settings: Grid Code → Poland). A third inverter, Z, was uninstalled from the prosumer photovoltaic installation site which was configured by the authorised installer and connected to the low-voltage network in 2020. The list of tested photovoltaic inverters is presented in Table 3.

Table 3. Tested photovoltaic inverters.

Inverter	Model	Type	Nominal Active Power	Other Parameters
X	SAJ Sununo Plus 3K-M	single-phase	3 kW	DC input: voltage range 80–600 V, MPPT (maximum power point tracking) voltage range 90–550 V, MPPT efficiency > 99.5%, current range 11 A AC output: rated voltage 230 V, rated current 13 A, power factor (full load) > 0.99, Euro efficiency 97.1%
Y	SAJ Suntrio Plus 5K	three-phase	5 kW	DC input: voltage range 150–1000 V, MPPT voltage range 160–900 V, MPPT efficiency > 99.9%, current range 11 A AC output: rated voltage 230 V/400 V, rated current 7.2 A per phase, power factor 0.9i–0.9c, Euro efficiency 97.2%
Z	GoodWe 5000 DT	three-phase	5 kW	DC input: voltage range 180–1000 V, MPPT voltage range 200–800 V, MPPT efficiency > 99.9%, current range 11 A AC output: rated voltage 230 V/400 V, rated current 8.5 A per phase, power factor 0.8i–0.8c, Euro efficiency 97.5%

The experimental platform for photovoltaic inverter tests was built in the Power Quality Laboratory of AGH University of Science and Technology in Cracow, Poland, based on the technical report IEC TR61000-3-15:2011 [35], specifying the low-frequency electromagnetic compatibility testing method for dispersed generation systems, and other similar experimental platforms presented in publications [36]. The experimental platform block diagram is shown in Figure 7.

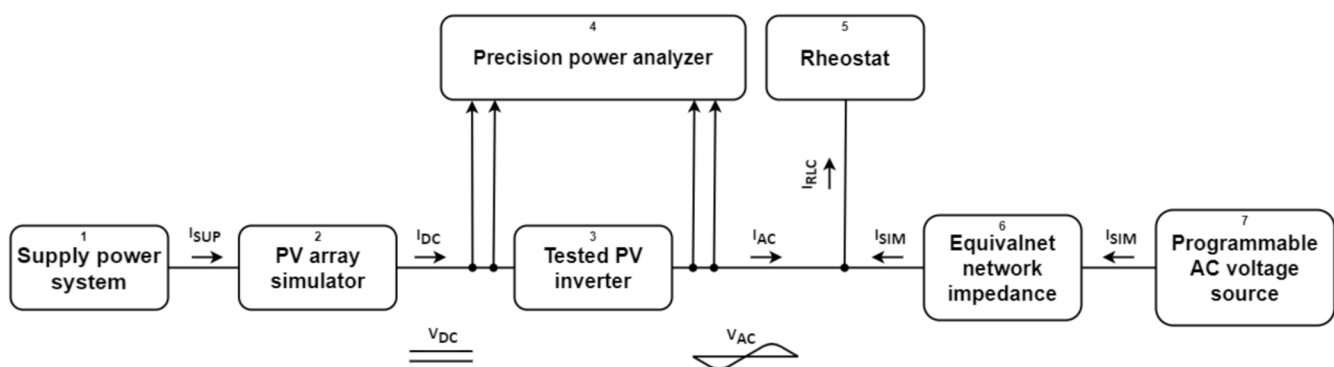


Figure 7. The simplified block diagram of the experimental platform.

The tested photovoltaic inverter (3) is supplied on the DC side by the photovoltaic array simulator (2) (DC source with adjustable current–voltage $I = f(U)$ characteristics). The inverter AC side is connected via a grid impedance element (6), with the resistance equal to 320 (m Ω) and the inductance equal to 1.43 (mH), to the electrical network simulator (7), a programmable AC source 3 \times 230 V, which allows for adjusting the voltage and the frequency at its output.

An additional element of the experimental platform is the regulated passive load (rheostat) (5), whose role is to balance the power generated by the tested inverter, thus it protects the electrical network simulator (7) from the power flow towards that device. On both sides of the tested inverter, powers, voltages and currents are measured using the

power analyser Yokogawa WT5000 (4). A picture of the experimental platform is shown in Figure 8 and an example of the current–voltage $I = f(U)$ characteristic is shown in Figure 9.

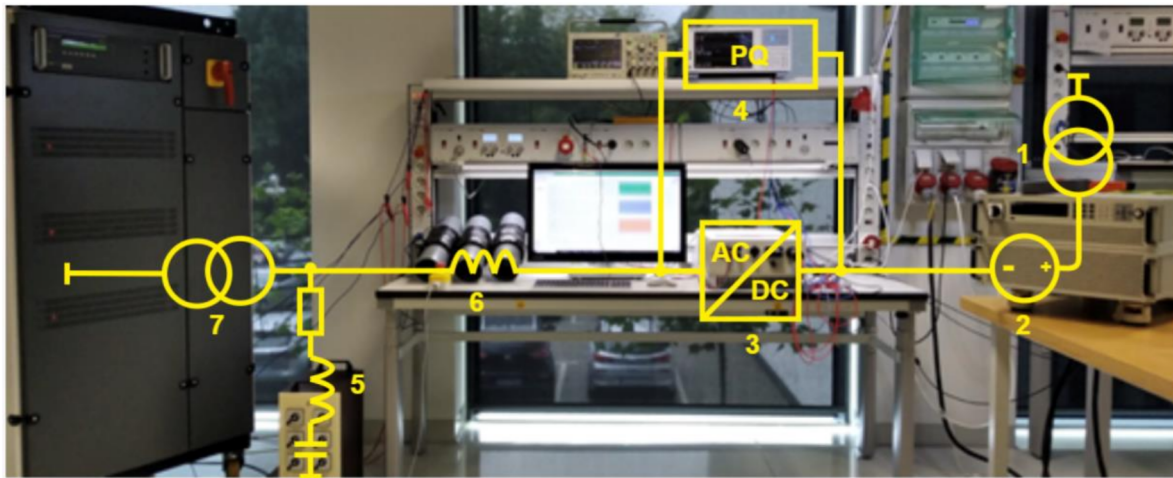


Figure 8. The laboratory stand for testing PV inverters at AGH University of Science and Technology (see Figure 7).

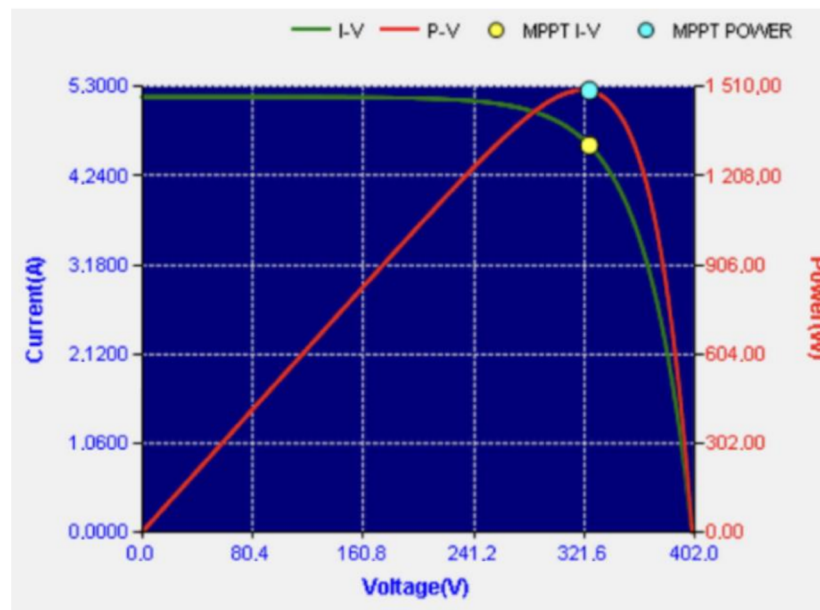


Figure 9. An example of the current–voltage $I = f(U)$ characteristic generated in the photovoltaic array simulator.

3.1. Test 1—Inverter Response to a Frequency Increase

The signal from the photovoltaic array simulator was supplied to the DC terminals of tested inverters in the form of current–voltage $I = f(U)$ characteristics corresponding to the DC active power of the photovoltaic array $P_{PV} = 1.5$ kW (for a single-phase inverter, X) and $P_{PV} = 1.25$ kW (for three-phase inverters, Y and Z). Then, after the inverters reached the steady state, corresponding to the maximum possible active power generation resulting from the previously set DC active power of the photovoltaic array P_{PV} , the frequency of the electrical network simulator was changed in the range of 50.0 to 51.9 Hz with a step of 0.1 Hz. For each frequency step, the values of test settings of frequency and DC power P_{DC} and measured results, AC active power P_{AC} , inverter efficiency η_e (2) and the maximum power point tracking (MPPT) efficiency η_{MPPT} (which was calculated by the photovoltaic array simulator) were measured and are collected in Appendix A: Table A1 (for the single-phase inverter X), Table A2 (for the three-phase inverter Y) and Table A3 (for

the three-phase inverter Z). Figure 10 presents the active power response to overfrequency of all tested photovoltaic inverters X, Y, Z.

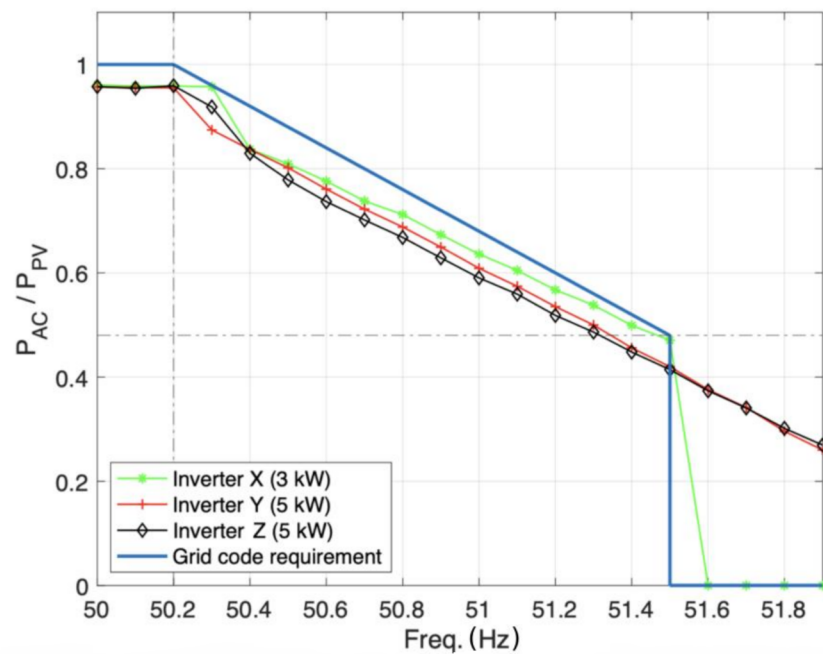


Figure 10. The active power frequency response to overfrequency for tested photovoltaic inverters X, Y, Z.

The η_e efficiency is calculated from the relationship:

$$\eta_e = \frac{P_{AC}}{P_{DC}} \quad (2)$$

The obtained results, which are collected in Tables A1–A3 and presented in Figure 10, indicate that all tested inverters responded to an increase in the frequency above 50.2 Hz with a decrease in the active power generation. Active power reduction in the range of 50.2–52 Hz corresponds to the requirements of the EU network code NC RfG [21]. For frequencies starting from 51.5 Hz, inverter X turned off, while inverters Y and Z continued to reduce active power generation according to the set 5% programmable droop. The operation of all three inverters is in accordance with the requirements of EU network code NC RfG [21] and the standard [22], because the minimum requirements presented in Table 1 allow an inverter to operate at frequencies greater than 51.5 Hz (there are no requirements for the operation time for frequencies greater than 51.5 Hz). The operation of the PV inverter X is not in accordance with the internal Polish DSOs' document [23], because it requires a PV inverter to continuously operate with overfrequency equal to 52 Hz.

The results presented in Tables A1–A3, especially the maximum power point tracking (MPPT) efficiency η_{MPPT} , show that limiting the active power generation with the increase in frequency is realised by shifting the operating point beyond the maximum active power point on the current–voltage $I = f(U)$ characteristic. An example of such an observation is presented in Figure 11.

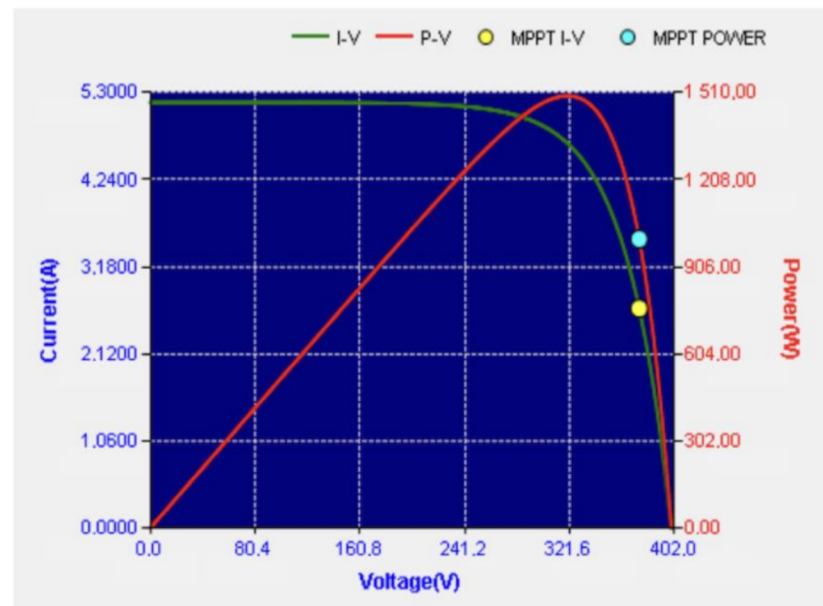


Figure 11. An example of the maximum power point tracking (MPPT) efficiency reduction resulting in the active power generation decrease.

A similar test, although limited to the frequency response, was conducted by Mastny et al. [30], who investigated six PV inverters from two manufacturers, two single-phase (with nominal power of 3.6 kW) and four three-phase PV inverters (with nominal power in the range of 3–10 kW). The experiment results showed that only one inverter fully complied with the EU network code NC RfG [21]. The remaining five inverters fulfilled the EU network code NC RfG [21] only partially or not at all. Their abnormal operation involved unfounded automatic disconnection from a network (one three-phase PV inverter), incorrectly performed frequency droop characteristic (four three-phase PV inverters) and a sudden drop in generated active power (one single-phase PV inverter and one three-phase PV inverter). One of the authors' conclusions is an urgent need for developing a certain verification mechanism for a large number of PV inverters that are connected to the electrical network.

3.2. Test 2 Inverter Response to a Voltage Increase

The signal from the photovoltaic array simulator was supplied to the DC terminals of tested inverters in the form of current–voltage $I = f(U)$ characteristics corresponding to the DC active power of the photovoltaic array $P_{PV} = 1.5$ kW (for a single-phase inverter, X) and $P_{PV} = 5$ kW (for three-phase inverters, Y and Z). The DC active power of the photovoltaic array P_{PV} corresponded to 50% and 100% of the inverter nominal active power for the single-phase inverter X and the three-phase inverters Y and Z, respectively. Then, after the inverters reached the steady state, corresponding to the maximum possible AC active power generation resulting from the photovoltaic array DC active power P_{PV} , the RMS voltage of the electrical network simulator was changed in the range of 230 to 260 V with a step of 5 V. For each voltage step, the values of DC power P_{DC} , AC active power P_{AC} , reactive power Q_{AC} , inverter efficiency η_e and the maximum power point tracking (MPPT) efficiency η_{MPPT} (which was calculated by the photovoltaic array simulator) were measured and are collected in Appendix B: Table A4 (for the single-phase inverter X), Table A5 (for the three-phase inverter Y) and Table A6 (for the three-phase inverter Z). Figure 12 presents the power displacement factor $\cos\phi$ response to a voltage increase for all tested photovoltaic inverters X, Y, Z.

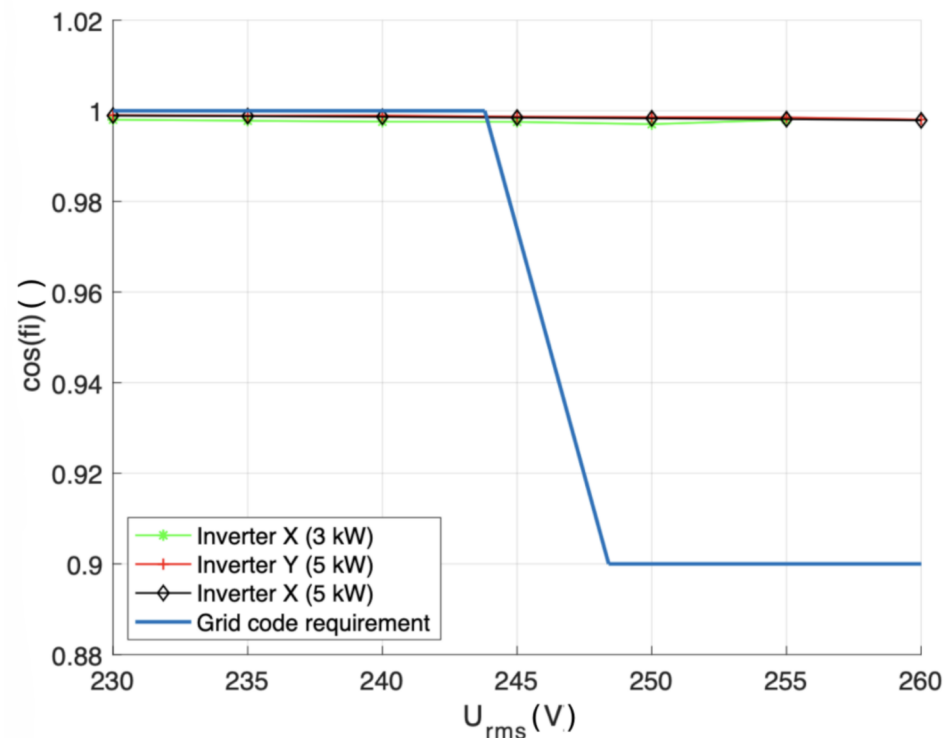


Figure 12. The power displacement factor $\cos\phi$ response to the voltage increase for all tested inverters X, Y, Z.

The obtained results, which are collected in Tables A4–A6 and presented in Figure 12, indicate that none of tested inverters responded correctly to the voltage increase by activating one of the permissible reactive power control modes, $Q = f(U)$ or $\cos\phi = f(P)$. The ability of inverters to operate in one of the mentioned reactive power control modes is very important for prosumers and DSOs, because it would decrease the number of automatic inverter shutdowns caused by overvoltage system protection activation and it would also decrease the number of consumer complaints.

3.3. Test 3—Inverter Active Power Generation Gradient After Automatic Reconnection After Tripping

The signal from the photovoltaic array simulator was supplied to the DC side of the tested three-phase inverters Y and Z in the form of current–voltage $I = f(U)$ characteristics corresponding to the DC active power of the photovoltaic array $P_{PV} = 5$ kW (which is equal to 100% of the inverter nominal active power). The total output AC active power measurements were carried out using a PQBOX-300 power quality analyser with 1 s mean RMS voltage and current aggregation time in order to measure the maximum active power gradient increase. The obtained results are shown in Figure 13.

According to the requirements presented in the EU network code NC RfG [21] and the standard [22], the permissible active power generation gradient growth shall not exceed 10% of the inverter nominal active power per minute. This means that the inverter nominal AC active power shall be achieved in 10 min. As can be seen in Figure 13, this requirement was only met by the inverter Z. The inverter Y reached its nominal AC active power in just 28 s, which does not fulfil the EU network code NC RfG [21] and the standard [22].

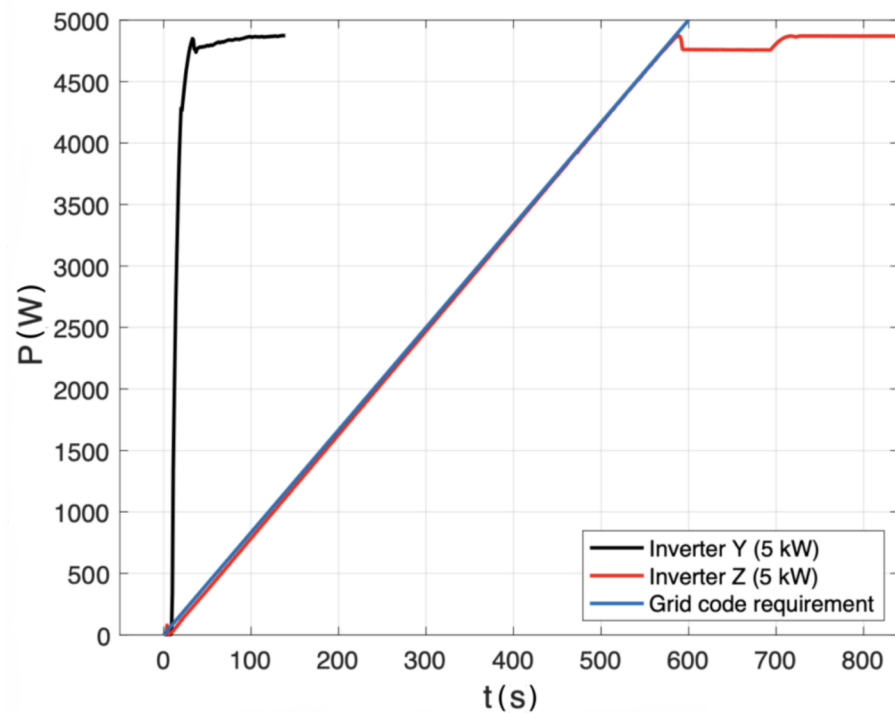
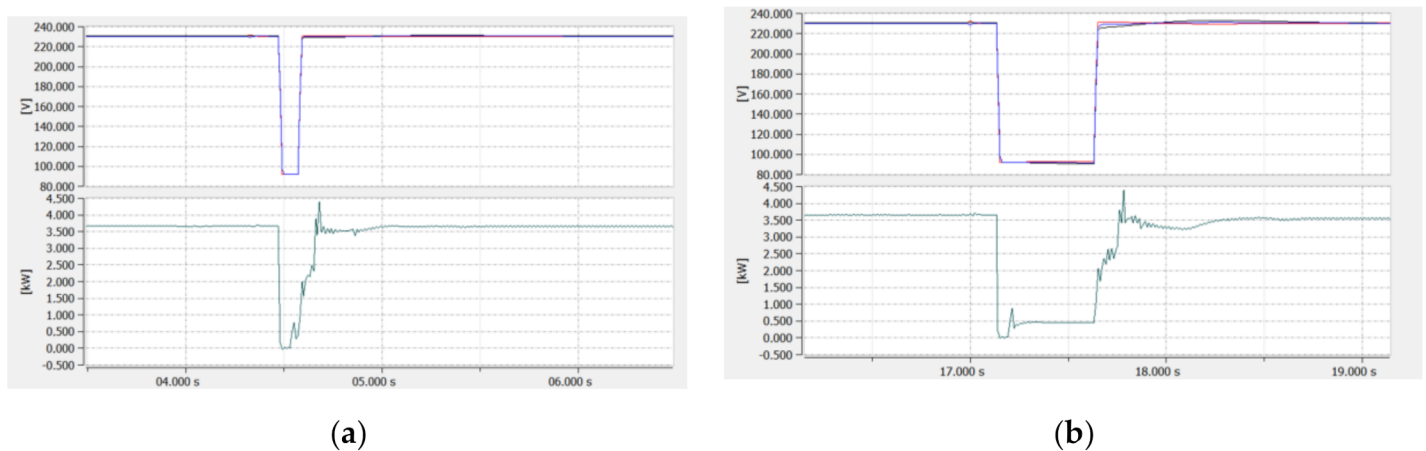


Figure 13. The measured active power generation gradients for tested Y and Z inverters.

3.4. Test 4—Inverter Immunity to Disturbances—Under-Voltage Ride Through (UVRT)

The under-voltage ride through (UVRT) requirement was checked for the inverters Y and Z. During the test, the signal from the photovoltaic array simulator was connected to the DC side of the tested inverters in the form of current–voltage $I = f(U)$ characteristics corresponding to the DC active power of the photovoltaic array $P_{PV} = 3.75$ kW (which is equal to 75% of the inverter nominal active power). The total output AC active power measurements were carried out using a PQBOX-300 power quality analyser with 10 ms RMS aggregation time. Recordings of AC voltages and output AC power during generated 60% depth voltage sag lasting 100 ms and 500 ms, i.e., events which were expected to be demanding for the inverters but located above the curve in Figure 6, are presented in Figures 14 and 15.



(a)

(b)

Figure 14. Inverter Y. AC voltages and output powers of the inverter Y during the 3-phase voltage sag of 60% depth and 100 ms duration (a) and 60% depth and 500 ms duration (b).

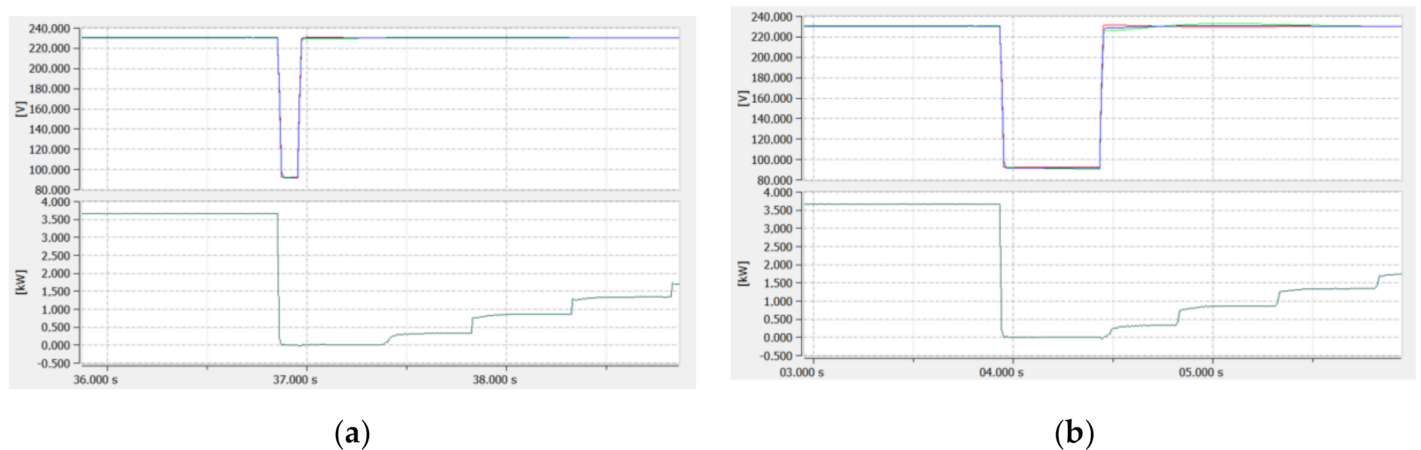


Figure 15. Inverter Z. AC voltages and output powers of the inverter Z during the 3-phase voltage sag of 60% depth and 100 ms duration (a) and 60% depth and 500 ms duration (b).

It can be seen that during both voltage sags, power generation of each inverter was reduced to zero, despite the fact that the residual voltage of the sag was 40% of the nominal voltage. This means that the power generation was stopped for a moment, however, none of the inverters was disconnected from the network or indicated any incorrect operation. After voltage returned to the nominal value, inverter Y during both voltage sags resumed full pre-fault power generation in less than 0.25 s, which fulfils the requirement resulting from the EU network code NC RfG [21] and the standard [22]. In turn, inverter Z did not meet this requirement for both voltage sags, since it needed approximately 10 s for resumption to 90% of pre-fault power, which is not as required by [21,22].

It is worth noting that the EU network code NC RfG [21] and the standard [22] do not define the active power generation drop during sag periods. As can be seen in Figure 14, despite the fact that power generation dropped to zero, operation of the inverter Y complies with the documents [21,22], where they only define how fast power generation should be resumed, but do not mention the maximum level of power generation drop. The authors can imagine a situation of a deep voltage sag on a high-voltage power line (e.g., caused by a lightning strike) that could cause the sudden and simultaneous power generation drop of thousands of photovoltaic micro-installations. That circumstance could lead to the situation that occurred in the United Kingdom (UK) on 9 August 2019 described in Section 2.3.

3.5. Test 5—Inverter Immunity to Disturbances—Rate of Change of Frequency (ROCOF)

The ROCOF immunity was checked for the inverters Y and Z. During the test, the signal from the photovoltaic array simulator was connected to the DC side of the tested inverters in the form of current–voltage $I = f(U)$ characteristics corresponding to the DC active power of the photovoltaic array $P_{PV} = 3.75$ kW (which is equal to 75% of the inverter nominal active power). The frequency and phase current (corresponding to active power) measurements were carried out using a PQBOX-300 power quality analyser with a 200 ms aggregation window. Inverters' responses to 0.5 Hz changes of frequency lasting 500 ms and 2500 ms, which correspond to 1 Hz/s and 0.2 Hz/s, respectively, are presented in Figures 16 and 17.

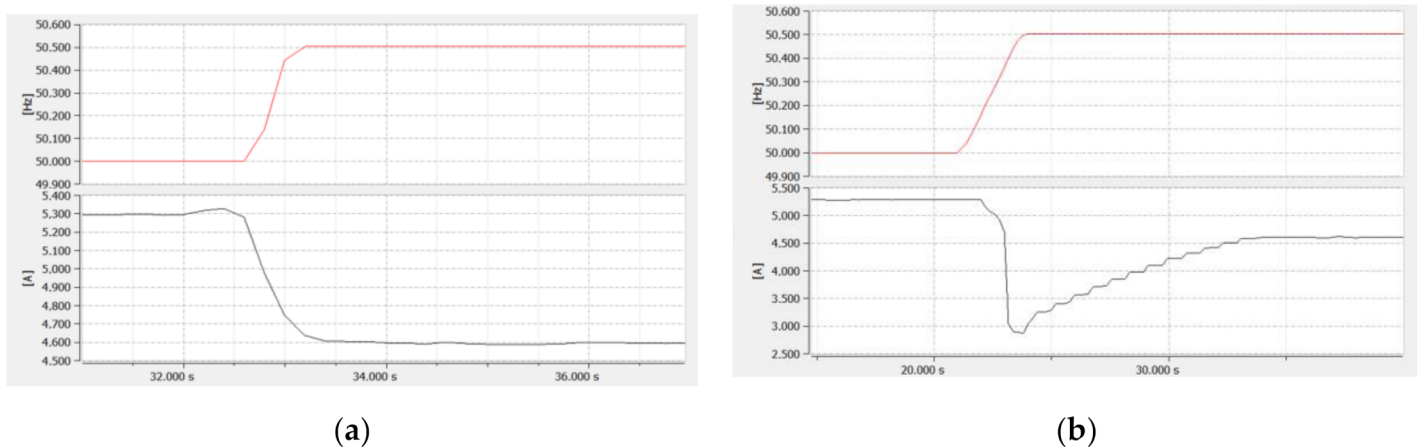


Figure 16. Inverter Y. Inverter Y response to 0.5 Hz/500 ms (a) and 0.5 Hz/2500 ms (b) change of frequency.

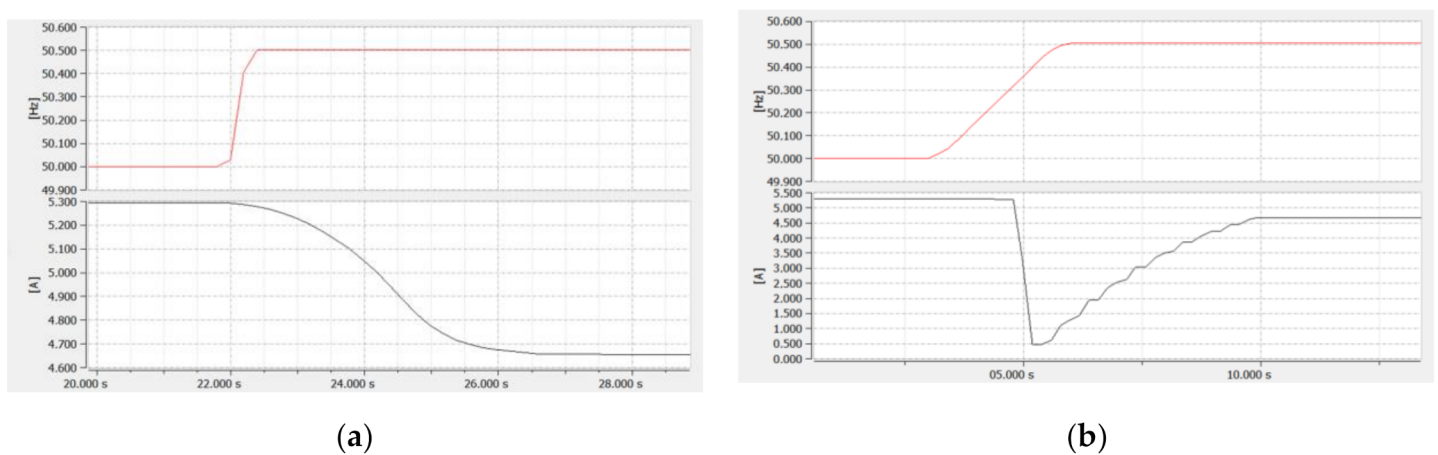


Figure 17. Inverter Z. Inverter Z response to 0.5 Hz/500 ms (a) and 0.5 Hz/2500 ms (b) change of frequency.

It can be seen that the rate of 0.5 Hz/500 ms (equal to 1 Hz/s) of change of frequency does not negatively affect the operation of the tested inverters. They continue power generation with a slight reduction as required by the EU network code NC RfG [21] and the standard [22]. The observation is different when the 0.5 Hz frequency change duration is longer over time, e.g., 2500 ms (equal to 0.2 Hz/s). For that case, both inverters reduce their power generation over 90% and need from 5 s to 5 min for power recovery. During the tests, none of the inverters was disconnected from the network or indicated any incorrect operation.

4. Conclusions

The paper presents selected PV inverters' requirements concerning photovoltaic micro-installation operation in low-voltage distribution networks in Poland and the EU. The laboratory test results of three, imported but widely available in the EU, low-price PV inverters are presented. The conducted tests have proven that, despite precisely defined technical requirements, the current formula for the connection procedure of PV micro-installations allows the connection of PV inverters that do not meet the requirements of the EU network code NC RfG [21], applicable standard [22] and internal DSOs' document [23]. Detailed results are as follows:

- all tested PV inverters (X, Y, Z) meet the EU network code NC RfG [21] requirement of operation in the active power output reduction mode (at the frequency threshold $f_1 = 50.2$ Hz and the programmable droop $s = 5\%$) in response to an increase in the network frequency (Figure 10);

- one tested PV inverter (X) does not meet the Polish DSOs' requirement [23] of operation in increased network frequencies (in the range of 51.5–52 Hz, Table 2), but it fulfilled the requirement of the EU network code NC RfG [21] (Table 1);
- all tested PV inverters (X, Y, Z) do not meet the Polish DSOs' requirement [23] of activating one of the permitted reactive power control modes against voltage level increase (Figure 12);
- one tested PV inverter (Y) does not meet the EU network code NC RfG [21] requirement of maintaining permitted power generation gradient after tripping (Figure 13);
- one tested PV inverter (Z) does not meet the EU network code NC RfG [21] requirement regarding under-voltage ride through (UVRT) immunity (it needed about 10 s to recover 90% of pre-fault power while 1 s is required, Figure 15);
- all tested PV inverters (X, Y, Z) meet the EU network code NC RfG [21] requirement regarding the rate of change of frequency (ROCOF) (Figures 16 and 17).

The authors also noticed and would like to highlight that the EU network code NC RfG [21] does not define the level of maximum active power generation drop during sag periods which, in the future, could be dangerous to sustaining the safety and reliable operation of a power system with a high concentration of PV micro-installations.

One of the main reasons why such PV inverters are still available on the market is the currently lack of the verification of photovoltaic inverters by independent accredited entities in terms of fulfilment of the requirements of the EU network code NC RfG [21], the standard [22] and the internal Polish DSOs' document [23]. In addition, lacking the reactive power control modes, which could limit the voltage rise phenomenon, has a negative impact on the low-voltage network's ability to absorb the energy produced from photovoltaic micro-installations, which results in more frequent photovoltaic inverter automatic shutdowns due to overvoltage protection system activation.

In order to reduce the number of PV inverter connections that do not fulfil the EU network code NC RfG [21], the standard EN 50549-1:2019 [22] and internal DSOs' requirements [23], the authors propose the following requirements:

- every PV inverter to be connected to the grid should be delivered with a valid certificate of compliance with the requirements considered in this paper and issued by the accredited EU entity;
- these declarations should clearly indicate the pre-set values of the PV inverter's protection system (its thresholds and tripping times) and the selected pre-set reactive power control mode, so as to give no doubts about expected inverter performance;
- the criteria for immunity verification of the inverter to a given grid disturbance, included in regulatory documents, should not only be focused on the assessment of whether the object maintains a connection to the grid, but should directly relate to its ability to maintain undisturbed generation during and after disturbance occurrence;
- DSOs from EU member states should develop and implement procedures of on-site PV inverter performance checks that could be applied during PV installation commissioning or complaint procedures.

There is no doubt that EU member states and DSOs, especially in the presently observed exponentially growing scale of PV micro-installation connections, should as soon as possible develop and implement at least the abovementioned actions that would contribute to eliminating from the EU market PV inverters that are not adapted to operate in EU power systems. One can only assume the scale of the problem and its future negative consequences (for consumers, TSOs and DSOs in the EU) in the current situation where the EU market has been flooded in recent years with PV inverters of unconfirmed and questionable performance.

Author Contributions: Conceptualisation, Z.H. and K.C.; methodology, K.C. and Ł.T.; validation, K.C., Ł.T. and A.P.; formal analysis, K.C., Ł.T. and A.P.; investigation, K.C., Ł.T. and A.P.; resources, K.C.; data curation, Ł.T. and A.P.; writing—original draft preparation, Ł.T.; writing—review and

editing, Z.H. and Ł.T.; visualisation, A.P.; supervision, K.C.; project administration, Z.H.; funding acquisition, Z.H. All authors have read and agreed to the published version of the manuscript.

Funding: This research was funded by the National Centre for Research and Development, grant number Gospostrateg1/385085/21/NCBR/2019.

Conflicts of Interest: The authors declare no conflict of interest.

Abbreviations

AC	Alternating current
c.a.	Circa
CE	Conformité Européenne
$\cos\varphi$	Displacement power factor
DC	Direct current
DSOs	Distribution system operators
EA	European co-operation for Accreditation
f	Actual network frequency
f_1	LFSM-O mode threshold activation
f_n	Nominal network frequency
I_{AC}	AC current supplied from the output of a tested PV inverter
I_{DC}	DC current supplied to the input of a tested PV inverter
I_{RLC}	AC current of rheostat
I_{SIM}	AC current supplied from the programmable AC voltage source
I_{SUP}	AC current supplied from the supply power system
LFSM-O	Limited frequency sensitive mode—overfrequency
MPPT	Maximum power point tracking
MV/LV	Medium voltage to low voltage
NC RfG	Network Code, Requirements for Generators
OFGEM	The Office of Gas and Electricity Markets
P, Q	Actual active and reactive power produced by a PV inverter
p.u.	Per unit
P_{AC}	AC active power at the output of a tested PV inverter
P_{DC}	DC active power at the input of a tested PV inverter
P_M	Active power generated at the output of a PV inverter at the network frequency f_1
P_n, Q_n	Nominal active and reactive power of a PV inverter
P_{PV}	DC active power at the output of the PV array simulator
PV	Photovoltaic
Q_{AC}	Actual reactive power at the output of a tested PV inverter
RED II	Renewable Energy Directive 2018/2001/EU
RES	Renewable energy sources
RMS	Root mean square
ROCOF	Rate of change of frequency
ROCOV	Rate of change of voltage
s	Programmable droop
t	Time in seconds
TSOs	Transmission system operators
U_{rms}	Actual RMS voltage at the output of a tested PV inverter's terminal
UE	European Union
UK	United Kingdom
U_n	Nominal RMS voltage of a distribution network
VOI	The ratio of voltage and current magnitude
η_e	Efficiency of a tested PV inverter
η_{MPPT}	MPPT efficiency

Appendix A

Table A1. The results of the inverter X's response to a frequency increase.

f [Hz]	P _{PV} [W]	P _{DC} [W]	η_{MPPT} [%]	P _{AC} [W]	η_e [%]	
50.0	1500	1499	99.99	1441	96.19	
50.1		1497	99.74	1438	96.11	
50.2		1496	99.74	1438	96.07	
50.3		1496	99.74	1436	96.01	
50.4		1301	86.87	1256	96.30	
50.5		1262	84.08	1214	96.26	
50.6		1209	80.62	1164	96.25	
50.7		1151	76.61	1107	96.09	
50.8		1107	73.65	1068	96.09	
50.9		1051	70.03	1010	95.98	
51.0		994	66.26	954	96.82	
51.1		947	63.16	907	95.75	
51.2		898	59.54	851	95.53	
51.3		845	56.14	807	95.51	
51.4		788	52.31	749	95.41	
51.5		741	49.36	706	95.28	
>51.6		Automatic inverter shutdown				

Table A2. The results of the inverter Y's response to a frequency increase.

F [Hz]	P _{PV} [W]	P _{DC} [W]	η_{MPPT} [%]	P _{AC} [W]	η_e [%]
50.0	1250	1247	99.72	1196	95.94
50.1		1245	99.84	1195	95.94
50.2		1244	99.59	1194	95.95
50.3		1141	91.10	1093	95.73
50.4		1094	88.35	1046	95.60
50.5		1048	84.04	1002	95.56
50.6		997	79.84	951	95.38
50.7		948	75.94	903	95.27
50.8		904	73.07	860	95.13
50.9		855	68.22	812	94.93
51.0		804	64.38	761	94.75
51.1		759	60.43	718	94.57
51.2		709	57.01	669	94.37
51.3		663	53.45	625	94.20
51.4		607	48.86	570	93.76
51.5		563	45.40	525	93.35
51.6		504	41.51	470	93.11
51.7		462	36.81	427	92.44
51.8		404	30.80	370	91.64
51.9	359	28.81	325	90.23	

Table A3. The results of the inverter Z's response to a frequency increase.

F [Hz]	P _{PV} [W]	P _{DC} [W]	η _{MPPT} [%]	P _{AC} [W]	η _e [%]
50.0	1250	1249	99.99	1197	96.08
50.1		1248	99.98	1193	96.09
50.2		1248	99.98	1199	96.09
50.3		1194	95.75	1148	96.13
50.4		1081	86.69	1037	95.98
50.5		1018	81.44	973	95.76
50.6		964	77.34	921	95.59
50.7		912	73.22	877	96.15
50.8		870	69.81	835	96.00
50.9		820	65.83	786	95.82
51.0		774	62.16	738	95.62
51.1		732	58.73	699	95.44
51.2		681	54.72	648	95.16
51.3		642	51.54	608	94.61
51.4		592	47.65	560	94.54
51.5		580	44.26	518	94.21
51.6		499	40.17	467	93.73
51.7		427	36.86	426	93.28
51.8		407	32.85	377	92.62
51.9		659	29.56	337	91.89

Appendix B

Table A4. The inverter X's response to the voltage increase.

U _{rms} [V]	P _{PV} [W]	P _{DC}	η _{MPPT} [%]	P _{AC} [W]	Q _{AC} [var]	η _e [%]
230	3000	2991	99.75	2874	−153	95.92
235		2996	99.94	2875	−149	95.98
240		2996	99.71	2873	−147	96.01
245		2991	99.88	2875	−146	96.04
250		2992	99.89	2874	−146	96.07
255		2989	96.11	2873	−147	96.09
260		2991	96.07	2873	−150	96.08

Table A5. The inverter Y's response to the voltage increase.

U _{rms} [V]	P _{PV} [W]	P _{DC}	η _{MPPT} [%]	P _{AC} [W]	Q _{AC} [var]	η _e [%]
230	5000	4979	99.64	4843	−213	97.25
235		4921	99.98	4855	−228	97.23
240		4994	99.82	4856	−223	97.28
245		4991	99.73	4845	−246	97.28
250		4993	99.84	4856	−256	97.30
255		4966	99.87	4860	−263	97.29
260		4644	92.29	4577	−285	97.21

Table A6. The inverter Z's response to the voltage increase.

U _{rms} [V]	P _{PV} [W]	P _{DC}	η _{MPPT} [%]	P _{AC} [W]	Q _{AC} [var]	η _e [%]
230	5000	4999	99.99	4.852	224	97.06
235		4999	99.99	4.853	−236	97.07
240		4999	99.99	4.854	−251	97.09
245		4999	99.99	4.853	−266	97.09
250		4999	99.99	4.853	−281	97.10
255		4999	99.99	4.851	−295	97.11
260		4999	99.99	4.855	−316	97.12

References

1. Electricity Price Statistics. Electricity Prices for Household Consumers. 2020. Available online: https://ec.europa.eu/eurostat/statistics-explained/index.php/Electricity_price_statistics#Electricity_prices_for_household_consumers (accessed on 28 December 2020).
2. Electricity and Heat Statistics. Consumption of Electricity and Derived Heat. 2020. Available online: https://ec.europa.eu/eurostat/statistics-explained/index.php/Electricity_and_heat_statistics#Production_of_electricity (accessed on 28 December 2020).
3. U.S. Energy Information Administration (EIA). Global Electricity Consumption Continues to Rise Faster Than Population. 2020. Available online: <https://www.eia.gov/todayinenergy/detail.php?id=44095> (accessed on 28 December 2020).
4. The International Energy Agency (IEA). Electricity Information: Overview. 2020. Available online: <https://www.iea.org/reports/electricity-information-overview> (accessed on 28 December 2020).
5. Regulation (EU) 2018/842 of the European Parliament and of the Council of 30 May 2018 on Binding Annual Greenhouse Gas Emission Reduction by Member States from 2021 to 2030 Contributing To climate Action to Meet Commitments under the Paris Agreement and amending Regulation (EU) No 525/2013. 2018. Available online: https://eur-lex.europa.eu/legal-content/EN/TXT/?uri=uriserv:OJ.L_.2018.156.01.0026.01.ENG (accessed on 28 December 2020).
6. European Union. The European Green Deal. Available online: https://ec.europa.eu/info/strategy/priorities-2019-2024/european-green-deal_en (accessed on 28 December 2020).
7. Directive 2009/28/EC of the European Parliament and of the Council of 23 April 2009 on the Promotion of the Use of Energy from Renewable Sources and Amending and Subsequently Repealing Directives 2001/77/EC and 2003/30/EC. 2009. Available online: <https://eur-lex.europa.eu/legal-content/EN/ALL/?uri=CELEX%3A32009L0028> (accessed on 28 December 2020).
8. European Union. Clean Energy for all Europeans Package. Available online: https://ec.europa.eu/energy/topics/energy-strategy/clean-energy-all-europeans_en (accessed on 28 December 2020).
9. Directive (EU) 2018/2001 of the European Parliament and of the Council of 11 December 2018 on the Promotion of the Use of Energy from Renewable Sources (Recast). 2018. Available online: https://eur-lex.europa.eu/legal-content/EN/TXT/?uri=uriserv:OJ.L_.2018.328.01.0082.01.ENG&toc=OJ:L:2018:328:TOC (accessed on 28 December 2020).
10. Polish National Fund for Environmental Protection and Water Management. Priority Programmes. Available online: <http://nfosigw.gov.pl/en/priority-programmes/> (accessed on 28 December 2020).
11. Priority Programme “My Electricity”. Available online: <https://mojprad.gov.pl> (accessed on 28 December 2020).
12. Księżopolski, K.; Drygas, M.; Pronińska, K.; Nurzyńska, I. The Economic Effect of New Patterns of Energy Efficiency and Heat Sources in Rural Single-Family Houses in Poland. *Energies* **2020**, *13*, 6358.
13. Bukowski, M.; Majewski, J.; Sobolewska, A. Macroeconomic Electric Energy Production Efficiency of Photovoltaic Panels in Single-Family Homes in Poland. *Energies* **2021**, *14*, 126. [CrossRef]
14. Polish National Fund for Environmental Protection and Water Management. News. Available online: <http://nfosigw.gov.pl/o-nfosigw/aktualnosci/art,1675,nfosigw-zwieksza-budzet-mojego-pradu-o-dodatkowe-100-mln-zl.html> (accessed on 28 December 2020).
15. Olczak, P.; Kryzia, D.; Matuszewska, D.; Kuta, M. “My Electricity” Program Effectiveness Supporting the Development of PV Installation in Poland. *Energies* **2021**, *14*, 231. [CrossRef]
16. Polskie Towarzystwo Przesyłu i Rozdziału Energii Elektrycznej (PTPiREE). Photovoltaic micro-installations in Poland. Available online: <http://www.ptpiree.pl/energetyka-w-polsce/energetyka-w-liczbach/mikroinstalacje-w-polsce> (accessed on 28 December 2020).
17. European Standard EN 50160:2010. *Voltage Characteristics of Electricity Supplied by Public Electricity Networks*; CENELEC: Rue de la science 23 Brussels, Belgium, 2010.
18. Fernandez, G.; Galan, N.; Marquina, D.; Martinez, D.; Sanchez, A.; Lopez, P.; Bludszuweit, H.; Rueda, J. Photovoltaic Generation Impact Analysis in Low Voltage Distribution Grids. *Energies* **2020**, *13*, 4347. [CrossRef]
19. Gandhi, O.; Kumar, D.S.; Rodriguez-Gallegos, C.; Srinivasan, D. Review of power system impacts at high PV penetration Part I: Factors limiting PV penetration. *Solar Energy* **2020**, *210*, 181–201. [CrossRef]
20. Patil, A.; Girgaonkar, R.; Musunuri, S.K. Impacts of Increasing Photovoltaic Penetration on Distribution Grid—Voltage Rise Case Study. In Proceedings of the 2014 International Conference on Advances in Green Energy, (ICAGE), Thiruvananthapuram, India, 17–18 December 2014.
21. Commission Regulation (EU) 2016/631 of 14 April 2016 Establishing a Network Code on Requirements for Grid Connection of Generators (NC RfG). 2016. Available online: https://eur-lex.europa.eu/legal-content/EN/TXT/?uri=OJ%3AJOL_2016_112_R_0001 (accessed on 28 December 2020).
22. Hes, S.; Kula, J.; Svec, K. Increasing DER Hosting Capacity in LV Grids in the Czech Republic in Terms of European Project InterFlex. In Proceedings of the 2019 International Conference on Smart Energy Systems and Technologies (SEST), Porto, Portugal, 9–11 September 2019.
23. Panda, G.; Jena, S.; Rangababu, P. A Low Voltage Ride Through Scheme for three phase grid connected PV inverter with an adaptive window based on MAF-PLL. In Proceedings of the 2018 8th IEEE India International Conference on Power Electronics (IICPE), Jaipur, India, 13–15 December 2018.

24. Buraimoh, E.; Davidson, I.E. Overview of Fault Ride-Through Requirements for Photovoltaic Grid Integration, Design and Grid Code Compliance. In Proceedings of the 2020 9th International Conference on Renewable Energy Research and Application (ICRERA), Glasgow, UK, 27–30 September 2020.
25. Karimi, M.; Farshad, M.; Hong, Q.; Laaksonen, H.; Kauhaniemi, K. An Islanding Detection Technique for Inverter-Based Distributed Generation in Microgrids. *Energies* **2021**, *14*, 130. [[CrossRef](#)]
26. Mastny, P.; Vojtek, M.; Moravek, J.; Vrana, M.; Klusacek, J. Validation of PV Inverters Frequency Response Using Laboratory Test Platform. In Proceedings of the 2020 21st International Scientific Conference on Electric Power Engineering (EPE), Prague, Czech Republic, 19–21 October 2020.
27. Great Britain's Electricity System Operator (National Grid ESO). Information about the 9 August 2019 Power Cut and the ESO. Available online: <https://www.nationalgrideso.com/information-about-great-britains-energy-system-and-electricity-system-operator-eso> (accessed on 28 December 2020).
28. Official UK Government Information Website. Available online: <https://www.gov.uk/government/publications/great-britain-power-system-disruption-review> (accessed on 28 December 2020).
29. Office of Gas and Electricity Markets (OFGEM), Information about the 9 August 2019 Power Cut. Available online: <https://www.ofgem.gov.uk/publications-and-updates/companies-pay-105-million-over-9-august-power-cut> (accessed on 28 December 2020).
30. IEC. *International Electrotechnical Commission (IEC) Technical Report IEC/TR 61000-3-15:2011 Electromagnetic Compatibility (EMC)—Part 3-15: Limits—Assessment of low Frequency Electromagnetic Immunity and Emission Requirements for Dispersed Generation Systems in LV Network*; IEC: Geneva, Switzerland, 2011.
31. Yu-Jen, L.; Pei-Hsiu, L.; Hong-Hsun, L. Grid-Connected PV Inverter Test System for Solar Photovoltaic Power System Certification. In Proceedings of the IEEE PES General Meeting Conference & Exposition, National Harbor, MD, USA, 27–31 July 2014.
32. Figueira, H.; Rech, C.; Schuch, L.; Hey, H.; Michels, L. Automated Test Platform for Grid-Connected PV Inverter Certification. In Proceedings of the IEEE 13th Brazilian Power Electronics Conference and 1st Southern Power Electronics Conference (COBEP/SPEC), Fortaleza, Brazil, 29 November–2 December 2015.
33. Wei, L.; Yanbo, Y.; Leijiao, G.; Wen, T. Automatic Test Platform for Photovoltaic Grid-connected Inverters. In Proceedings of the 5th International Conference on Power Electronics Systems and Applications (PESA), Hong Kong, China, 11–13 December 2013.
34. Zhao, X.; Jin, Y. Development of a Test Platform for Grid-connection PV Systems. In Proceedings of the Asia-Pacific Power and Energy Engineering Conference, Wuhan, China, 25–28 March 2011.
35. Bravo, R.J.; Yinger, R.; Robles, S. Three phase solar photovoltaic inverter testing. In Proceedings of the 2013 IEEE Power & Energy Society General Meeting, Vancouver, BC, Canada, 21–25 July 2013.
36. Kafle, Y.R.; Town, G.E.; Guochun, X.; Gautam, S. Performance comparison of single-phase transformerless PV inverter systems. In Proceedings of the 2017 IEEE Applied Power Electronics Conference and Exposition (APEC), Tampa, FL, USA, 26–30 March 2017.